



Contents lists available at [SciVerse ScienceDirect](#)

Journal of Analytical and Applied Pyrolysis

journal homepage: www.elsevier.com/locate/jaap



Production of char from vacuum pyrolysis of South-African sugar cane bagasse and its characterization as activated carbon and biochar

Marion Carrier^a, Ailsa G. Hardie^b, Ümit Uras^a, Johann Görgens^a, Johannes (Hansie) Knoetze^{a,*}

^a Department of Process Engineering, University of Stellenbosch, Private Bag X1 Matieland, 7602, South Africa

^b Department of Soil Science, University of Stellenbosch, Private Bag X1 Matieland, 7602, South Africa

ARTICLE INFO

Article history:

Received 11 November 2011

Accepted 26 February 2012

Available online xxx

Keywords:

Sugar cane bagasse

Vacuum pyrolysis

Steam activation

Activated carbon

Biochar

ABSTRACT

The potential of vacuum pyrolysis to convert sugar cane bagasse into char materials for wastewater treatment and soil amendment is the focus of this research paper. Vacuum pyrolysis produces both bio-oil and char in similar quantities. Vacuum pyrolysis has the potential to produce high quality chars for wastewater treatment and soil amendment directly during the conversion process, with no further upgrading required. In the present study, chars with the required porous structure was obtained directly from the vacuum pyrolysis process, making it very efficient as adsorbent both in terms of methylene blue (MB) adsorption with a N_2 -BET surface area of $418 \text{ m}^2 \text{ g}^{-1}$. Further steam activation of the chars benefited the development of meso- and macroporosity, although this upgrading step was not essential to achieve the required performance of char as an MB adsorbent. The development of large pores during the vacuum pyrolysis favored physisorption of MB, rather than chemisorption. The chemical nature of the vacuum pyrolysis char resulted in a slightly acidic surface (pH 6.56). The biochar from vacuum pyrolysis can be considered as a highly beneficial soil amendment, as it would enhance soil nutrient and water holding capacity, due to its high cation exchange capacity ($122 \text{ cmol}_c \text{ kg}^{-1}$) and high surface area. It is also a good source of beneficial plant macro- and micronutrients and contains negligible levels of toxic elements.

© 2012 Published by Elsevier B.V.

1. Introduction

Sugar cane bagasse (SB) is one of the main biomass wastes from sugar production and represents 30–40 wt.% of these wastes [1]. In 2008, South Africa produced 7.9 million tonnes of bagasse [2]. This valuable waste is intensively used in different contexts in South Africa. For the sugar industries, this waste is mainly converted into energy through combustion [3]. Applications in pulping [4], activated carbon production [5,6], cellulosic ethanol production [7] and energy production through pyrolysis [8] and gasification [9] have been considered in South Africa.

Pyrolysis is a thermochemical process used to convert biomass into energy-dense bio-fuels namely biochar, bio-oil and non-condensable gases. Different types of thermochemical decomposition such as gasification, pyrolysis, torrefaction and combustion produce different product qualities and ratios by controlling the process conditions. Fast pyrolysis is optimized for high liquid yields; gasification maximizes gas production; vacuum pyrolysis gives a more even spread of products; slow pyrolysis and torrefaction give char as main product; and finally combustion produces heat [10]. A previous study demonstrated the

advantages of vacuum pyrolysis, compared to conventional slow pyrolysis [8]. Bio-oil production increased during vacuum pyrolysis, reaching $23.6 \pm 4.3 \text{ wt.}\%$ compared to $18.7 \pm 5.0 \text{ wt.}\%$ from slow pyrolysis, while the opposite trend was observed for char production, $18.8 \pm 0.3 \text{ wt.}\%$ and $29.4 \pm 0.3 \text{ wt.}\%$ for vacuum and slow pyrolysis, respectively [8]. Slow pyrolysis typically produces three valuable products in the following ranges: 35% of char, 30% of liquid (oil + water) and 35% of gas, compared to 10% of char, 65% of liquid and 25% of gas for fast pyrolysis [11]. In the case of vacuum and slow pyrolysis, the production of three valuable products is expected while the production of liquid is maximized in fast pyrolysis. These last products from fast [12,13], slow [8,14] and vacuum [8,15,16] pyrolysis of SB have been used to produce bio-oil, char and gases for chemicals, adsorbents, soil amendments and energy. In particular, the production of activated carbon (AC) from SB has been extensively investigated [5,14,17–21], while the utilization of SB biochar as a soil amendment has not received much attention [22].

The present study will focus on the characterization of char from vacuum pyrolysis for possible application as soil amendment and will compare its adsorptive properties to activated carbon produced by steam gasification of the same char. This comparison should conclude whether a single step vacuum pyrolysis process would be sufficient to produce chars with properties required for soil amendment, or whether a second steam activation step

* Corresponding author. Tel.: +27 021 808 4488; fax: +27 021 808 2059.

E-mail address: jhk@sun.ac.za (J. Knoetze).

is required. Currently research scientists are using a large range of analytical techniques to determine the physico-chemical properties of char materials, aimed at explaining the adsorption phenomena. There are two kinds of adsorption, namely physisorption which is caused by van der Waals – and electrostatic forces and chemisorption, which involves formation of a chemical. Many studies have been carried out on the MB adsorption on low-cost adsorbents [23]. Most of the studies on Methylene Blue (MB) adsorption combined the experimental results with BET measurements and adsorption models to point out possible mechanisms [24,25]. Rafatullah et al. [23] speculated on the possibility of the ion exchange mechanism (physisorption) involved in MB uptake. In the second part of the paper, the materials produced will be considered as soil amendments. The mechanisms of biochar reactions on soils are really complex as discussed by Joseph et al. [26]. The initial reactions of biochar when placed in soil, can be classified as dissolution-precipitation reactions (pH, cation exchange capacity, electrical conductivity, ash content, acidity and alkalinity properties involved), redox reactions (carbon content involved), acidic and basic surface charge of biochars, sorption of organic compounds on biochar surfaces (BET and MB involved), biochar–soil mineral–soil organic–matter interactions, macropore filling and interactions with micro-organisms and dissolved organic matter and minerals. However, a series of analyses have been selected to point out the basic biochar characteristics which are critical to obtain a valuable soil amendment [27].

The pH, cation exchange capacity (CEC) [28,29] and electrical conductivity (EC) [30] of the biochar depend on both the content and composition of the mineral fraction [31,32]. The water and citric acid-extractable nutrients give an indication of biochar's essential nutrient and toxic element content. The content of water-soluble sodium may affect clay dispersion (ultimately soil structure) and plant growth [33]. The water and citric acid availabilities of nutrients in biochars are related to the type of bonds associated with the elements involved. The presence of this range of reactive functional groups can be qualitatively identified by FT-IR [34] and quantified by the determination of the acidity and alkalinity of the surfaces [35,36].

This study is intended for a rapid characterization of materials, char and activated carbons from vacuum pyrolysis and steam gasification, respectively, and will compare their adsorptive characteristics in the first part while the char from vacuum pyrolysis will be considered as soil amendment in the second part.

2. Materials and methods

2.1. Biomass

The sugar cane bagasse was provided by the Sugar Milling Research Institute in Durban (South Africa). The bagasse was stored indoors while the experiments were conducted. The bagasse was dried for three days at ambient temperature. Before vacuum pyrolysis, the material was milled in a Retsch ZM200 mill and sieved through a JEL (J. Engelsmann) sieve machine for 10 min. Fractions with particle diameters in the range of 425–850 μm were selected for experimental work.

2.2. Vacuum pyrolysis set-up

The pyrolysis reactor consisted of a 1 m long, 60 mm OD quartz tube, heated by six well insulated, computer controlled heating elements. The heated chamber was connected to a condensation train and a vacuum pump. The pipes leading from the reactor to the condensation train was maintained at 100–120 °C to limit condensation before the traps. The vacuum pump removed the organic

vapors and gas products from the reactor through the condensation train. The condensable gasses were then condensed in the vacuum traps and recovered as liquid, which were later weighed and analyzed. The condensation train consisted of five condensers; the first was held at room temperature, the second and third at –10 °C and the last two at –55 °C (dry ice temperature). A control program was designed to control the heating rate, pyrolysis time and final pyrolysis temperature. Once the reaction finished, the set-up was allowed to cool under vacuum until the sample temperature was below 120 °C. The sample holder was then removed and weighed, after which the residue (char) was removed and stored for analysis. A typical run would last between 2 and 3 h, after which the reactor was allowed to cool for ± 2 h depending on the pyrolysis temperature employed. A good compromise between yield and quality of products from SB (40 g) pyrolysis has been obtained with the following experimental conditions: a temperature of 460 °C, a heating rate of 17 °C min^{–1}, a pressure of 8 kPa_{abs} and a hold time of 1 h. These experimental conditions allowed maximizing the Brunauer, Emmett and Teller (BET) surface area of the chars [8]. The yields of char, bio-oil, pyrolytic water and gas from vacuum pyrolysis of sugar cane bagasse are 18.1 \pm 2.7, 22.0 \pm 3.1, 19.1 \pm 2.3 and 30.8 \pm 4.9 wt.%, respectively [8].

2.3. Activation set-up

For activation experiments, an apparatus based on the thermogravimetric analysis (TGA) principle at Potchefstroom Campus of North-West University (South Africa) was used. Isothermal thermal gasification experiments of in situ chars were conducted during the study. A mixture of 60 mol% steam and nitrogen flow of 350 L h^{–1} were introduced into the TGA. After the apparatus was stabilized under the desired operating conditions, the furnace was elevated and the biochar sample was placed into the sample holder. Due to the high heterogeneity of biochars and despite their low density, a sample weight of 1 g was used during each experiment. After a part of the carbon content was converted (approximately 1 h) the char sample was cooled in an inert atmosphere. Blank experiments were carried out to determine the effects of heating alone. Char placed in a nitrogen atmosphere was heated under the same experimental conditions as those adapted for the activation experiments.

In the gasification step, the steam reacts with the carbon to produce CO, CO₂, H₂ and CH₄. This process is referred as 'burn-off', where the carbon content of the char is reduced by reaction with the steam. Consequently, the amount of carbon produced was markedly reduced during activation. Heat treatment alone led to burn-off of about 22.5% and 37.7% at 800 and 900 °C respectively in comparison to 54.5, 61.7 and 65.1% with steam at temperatures of 700, 800 and 900 °C, respectively.

2.4. Physical and chemical characterization of char as activated carbon and soil amendment

2.4.1. Moisture and ash contents

Moisture and ash contents analyses were done by heating the samples in air to 105 °C for 24 h and to 575 \pm 20 °C for 4 h, respectively, and weighing the residue.

2.4.2. Total elemental analysis

The total content of C, N and H were determined using a dry-combustion method using Eurovector CNH analyzer. The O + S content was determined by subtracting the ash and C, N and H contents from the total mass of the sample. Major (Na, Mg, Si, K, Ca, Ti, Mn, P, Al, Cr and Fe) and trace elements (Cr, Ni, Zn, As, Ga, Co, V, Rb, Sr, Y, Zr, Nb, Ce, Nd, La, Th, U, Ba, S and Cl) of the raw materials were determined by X-ray fluorescence (XRF, PANalyticalAxios).

2.4.3. Proximate analysis

Proximate analysis was performed with a thermogravimetric method (PerkinElmer Pyris TGA 7). The sample was heated from 25 °C to 600 °C at 10 °C min⁻¹ and then from 600 °C to 900 °C at 20 °C min⁻¹ under nitrogen. After 7 min, oxygen at a 15 mL min⁻¹ flow rate was introduced for the combustion stage during 1 h at 900 °C.

2.4.4. BET specific surface area and microporosity

The surface area of the charcoal was determined using the multipoint BET analysis on a Micrometrics ASAP 2010 system. Once degassed on a VacPrep 061 system at 300 °C, the sample was introduced to the N₂ adsorption equipment.

2.4.5. Methylene blue adsorption

Concentrations of 1.0–20.0 mg L⁻¹ of methylene blue (MB) were made up and their absorbance measured at 630 nm on a Biochrom System Ultraspec 1000 UV/visible spectrophotometer. The maximum absorbance of MB is obtained at 630 nm at a pH around 5 [33]. The calibration curve of absorbance against concentration of MB was determined and indicated that the Beer–Lambert law is obeyed up to a concentration of 20 mg L⁻¹. To determine the adsorption of MB on activated carbon, on average 0.2 g (weighed with precision on a Denver Instrument balance) of material were added to 50 mL of 20 mg L⁻¹ MB solution and stirred on a magnetic stirrer (MSH 300 Boeco model) at a speed of 6 rpm. Aliquots were taken at intervals during a 15 min period, filtered on Whatman filter paper, introduced in disposable cuvettes (PMMA 2.5 mL macro, PlastiBrand) and the absorbance of the suspensions determined. An absorbance value of 2.06 ± 0.02 was obtained for the initial solution of MB. The temperature and pH were measured during the adsorption experiments using a 827 Metrohm pH lab system. The char and activated carbons were compared to two commercial activated carbons, Diahope CQ Cane activated carbon (Iodine number: 1050 mg g⁻¹; specific surface area: 1150 m² g⁻¹) and Chemviron Cane CAL (Iodine number: 1000 mg g⁻¹; specific surface area: 1050–1100 m² g⁻¹), produced from selected grades of bituminous coals.

2.4.6. pH of biochar in water and 1 M KCl

The pH of biochar was determined according to Novak et al. [35] and Cheng and Lehmann [36]. Two grams of biochar were shaken (IKA®KS 260) with 40 mL distilled water or 1 M KCl (99% of purity, Merck Chemicals Ltd.) solution for 30 min. This suspension was allowed to stand for 10 min before measuring the pH with a pH electrode 827 pH Lab (Metrohm).

2.4.7. Cation exchange capacity (CEC)

Determination of the CEC of char gives an indication of the abundance of negatively charged sites on the biochar which can retain exchangeable cations that are essential plant macronutrients, e.g. NH₄⁺ and Ca²⁺. It is based on the method by Rhoades [29] as it is suitable for materials with a wide pH range. Firstly, the biochar is saturated with a buffered solution of NaCl (99.9% of purity, Hopkin & Williams Ltd.) adjusted to pH 7.0. This involves placing 1 g of ground biochar in a 30 mL centrifuge tube and adding 20 mL of the saturating solution (0.4 N NaOAc–0.1 N NaCl, 60% ethanol solution (99.9% of purity, United Scientific Ltd.) adjusted to pH 7.0 using 3 M HCl (Merck Chemicals Ltd.)). The tube is sealed and shaken for 1 h. It is then centrifuged to separate the biochar from the liquid, and the supernatant is discarded. This procedure is repeated three times to ensure complete saturation of cation exchange sites with Na⁺. The Na/Cl molar ratio of the saturating solution has to be determined using ion chromatography (Dionex DX-120 Ion Chromatograph).

Secondly, the Na is exchanged with Mg. This involves adding 20 mL of extracting solution 0.25 M Mg(NO₃) (99.9 of purity, United

Scientific Ltd.) to the Na saturated biochar and shaking for an hour. The suspension is then centrifuged and the supernatant is decanted into a 100 mL volumetric flask. This extraction procedure is repeated twice with fresh extracting solution to ensure that all Na is exchanged and extracted. The collected supernatants are then made up to a volume of 100 mL using distilled water. The Na (Na_t) and Cl (Cl_t) concentration in the solution is determined using ion chromatography. The CEC (cmol_c kg⁻¹) is calculated by determining the total amount of exchangeable Na as follows:

$$\text{Exchangeable Na (cmol kg}^{-1}\text{)}$$

$$= [(Cl_t) \times (Na/Cl) \text{ saturating solution}]$$

2.4.8. Surface acidity and alkalinity using Boehm titration method

Boehm titration provides an indication of the total surface acidity and alkalinity of the biochar, and is based on the method described by Cheng and Lehmann [36]. A 0.15 g subsample of biochar was added to 15 mL of either 0.1 N NaOH or 0.1 N HCl solution (Merck Chemicals Ltd.) and shaken with an end-over-end shaker for 30 h. The biochar slurry was then filtered using a Whatman no. 40 filter paper. An aliquot of 5 mL of the NaOH filtrate was transferred to a 10 mL 0.1 N HCl solution that neutralized the unreacted base. The solution was back-titrated with 0.1 N NaOH with a phenolphthalein (PAL Chemicals) indicator. Surface basicity was measured similarly to the measurement of surface acidity and an aliquot of 5 mL of the HCl filtrate was directly titrated with 0.1 N NaOH. The base or acid uptake of BC was converted into the content of surface acidity or surface basicity (mmol g⁻¹), respectively.

2.4.9. Water soluble nutrients and electrical conductivity

The water soluble anions (NO₃⁻, PO₄³⁻, Cl⁻, F⁻, SO₄²⁻) and cations (Ca²⁺, Mg²⁺, Na⁺, K⁺) were extracted using a 1:20 (w/w) mixture of biochar in distilled water. The solution was shaken for 1 h and the suspension filtered. The electrical conductivity was measured (Jenway, 4510 conductimeter) and anion and cation concentrations determined using an ion chromatograph (Dionex DX-120 Ion Chromatograph).

2.4.10. Citric acid-extractable nutrients

Extractable nutrients concentrations in biochar were determined by Inductively Coupled Plasma-Mass spectrometer (ICP-MS is an Agilent 7700) for macro-elements and ICP-AES analysis for microelements (Varian Liberty II Radial ICP instrument) after wet-digestion in 1% citric acid (>99.7% of purity, Glenvista). Warmed (80 °C) 1% citric acid (20 mL) was added to weighed solid sample (1 g) into 100 mL volumetric flasks. The solutions were heated until 80 °C and shaken every 10 min. Solutions were filtered through ash-less filter (Whatman filter papers no. 40) before the ICP-MS analysis.

2.4.11. FT-IR analysis

Dried biochar samples were mixed with spectrograde KBr (Merck Chemicals Ltd.) at the ratio of 1:200 (w/w) and the mixture was hydraulically pressed. The pellets were analyzed by using ThermoFinnigan Nexus 6700 FTIR spectroscopy. The OMNIC® software package which automatically corrects the medium's background material was used to measure the FTIR spectra.

3. Results and discussion

3.1. Characterization of materials as activated carbon

3.1.1. Elemental and proximate analyses

The comparison of the elemental and proximate analyses between initial biomasses, char and AC indicated a gradual increase in carbon content explained by the release of the organics rich

Table 1
Elemental and proximate analyses of initial bagasse, char (C) and activated carbon (AC) from vacuum pyrolysis and steam gasification. WC: water content; VM: volatile matter and FC: fixed carbon.

| Material | Ash (900 °C) | C (wt.%) | N (wt.%) | H (wt.%) | O + S ^a (wt.%) | WC (wt.%) | Ash (850 °C) | VM (dry,wt.%) | FC ^a (dry, wt.%) |
|-----------|--------------|-----------|----------|----------|---------------------------|-----------|--------------|---------------|-----------------------------|
| Bagasse | 3.1–3.5 | 45.8–52.7 | 1.0 | 5.1–5.8 | 45.0–37.0 | 8.8 | 5.6 | 82.5 | 11.9 |
| C-460 °C | 11.9–16.4 | 60.4–65.3 | 0.8–1.0 | 1.5–2.2 | 25.4–15.1 | 7.7 | 14.8 | 57.3 | 36.2 |
| AC-700 °C | 22.0 | 73.6 | 0.7 | 0.6 | 3.1 | 2.9 | 22.7 | 21.7 | 58.6 |
| AC-800 °C | 16.1 | 77.9 | 0.9 | 0.6 | 4.5 | 4.6 | 16.9 | 19.0 | 69.0 |
| AC-900 °C | 12.2 | 78.2 | 0.6 | 0.5 | 8.5 | 4.8 | 12.8 | 19.5 | 72.7 |

^a Obtained by difference.

in H and O contents during the volatilization and activation steps (Table 1). As the trends in ash, H and O + S contents were not consistent due to the inhomogeneity of materials, it was not possible to draw specific conclusions with regard to H and O + S contents. Nevertheless, a general decrease in H and O + S contents was observed after both the pyrolysis and activation steps.

The high C:N ratio of the biochar, 53.4–61.5 (Table 1), would imply that the addition of the biochar to soil would lead to the immobilization of soil nitrogen and a soil nitrogen deficiency induced by microbial assimilation of all available soil N to break down C-rich substrate, which would have a negative impact on the growth of plants [37]. However, since much of the C in biochar is condensed, aromatic types of C that are considered as very difficult for soil microorganisms to degrade [38], it is doubtful that the biochar would cause significant immobilization of nitrogen. However, it is recommended that biochar should not be applied to soil without the addition of N fertilizer, as it is not balanced in terms of its elemental content. The low moisture content of char does not affect the adsorptive power and make it commercially viable as the requirements are generally stipulated between 3–10 wt.% [39].

A weight loss of 80.7% took place during the pyrolytic step at 200–460 °C (results not shown). As reported, this low-temperature region coincides with the alkali metal release emitted in connection with the decomposition of the organic structure pointed out by the release of O and H contents (Table 1) [40]. The release of alkali and alkaline earth metals (AAEM) and subsequent decrease of ash content with the increasing activation temperature (Table 1) have also been reported for the steam gasification of Eucalyptus chips [41]. The presence of the steam at higher temperature will therefore advance the devolatilization of inorganics, especially the AAEM, released with the tar. It is possible that the fine particles are AAEMs produced by the cleavage of chemical bonds containing AAEM species, e.g. –OM and –COOM (M = K, Na, Ca, and Mg), with steam [41].

The high volatile content makes biomass chars much more reactive for a steam gasification purpose than those of lignite and hard coal [42]. Major proximate components of biomass are volatiles which are discharged during the pyrolytic step, from 82.5 wt.% to 57.3 wt.% (Table 1). The steam gasification step released a larger amount of volatiles (Table 1), which should be correlated to the BET surface area increase.

Table 2
Porous characteristics of char and activated carbons.

| Bagasse | BET SA (m ² g ⁻¹) | BO (%) | Micropore V (cm ³ g ⁻¹) | Micropore A (m ² g ⁻¹) | SP Total V. of pores (cm ³ g ⁻¹) |
|----------------------------|--|--------|--|---|---|
| C (460 °C) | 259 | – | 0.088 | 194.0 | 0.136 |
| C (800 °C/N ₂) | 349 | 22.5 | 0.139 | 306.0 | 0.174 |
| C (900 °C/N ₂) | 452 | 37.7 | 0.168 | 369.0 | 0.258 |
| AC (700 °C/Steam) | 441 | 48.1 | 0.181 | 399.9 | 0.189 |
| AC (800 °C/Steam) | 570 | 61.7 | 0.157 | 345.6 | 0.356 |
| AC (900 °C/Steam) | 561 | 54.5 | 0.131 | 289.0 | 0.526 |
| Diahope | 1152 | – | 0.254 | 578.7 | 0.705 |
| Chemviron | 984 | – | 0.293 | 646.8 | 0.590 |

Burn-off (BO), single point (SP), char (C), activated carbon (AC), A: area, V: volume.

3.1.2. BET surface area

Any supplementary treatments applied on the char (BC), gasification or/and steam activation (gasification) increased the BET surface areas (Table 2). The surface areas of ACs obtained at 700 °C were lower than those treated at 800 and 900 °C. For instance, the surface area were 391–441 m² g⁻¹ and 561–570 m² g⁻¹ for the activated carbons from bagasse after 1 h of activation at 700 and 800–900 °C, respectively (Table 2).

The BET surface areas of AC obtained from activation of chars were lower than those reported previously, including Devnarain [5] (806 m² g⁻¹; pyrolysis 500 °C, 10 °C min⁻¹; activation: steam 13 g min⁻¹, 800 °C, 20 min), Bernardo et al. [19] (761 m² g⁻¹; pyrolysis 680 °C, 10 °C min⁻¹, 1 h; activation: steam 6.4 g min⁻¹, 800 °C, 4 h) and Jaguaribe et al. [43] (931–1397 m² g⁻¹; pyrolysis 300 °C, 1 h; activation: steam 3 g min⁻¹, 800 °C, 1.5 h). The maximum BET surface area reached in this study is 570 m² g⁻¹ from the vacuum pyrolysis of milled and sieved bagasse (pyrolysis 460 °C, 17 °C min⁻¹, 8 kPa; activation: steam 6.4 g min⁻¹, 800 °C, 1 h). As illustrated above, wide variations exist in the experimental conditions that are employed in the different studies, which make comparisons difficult. Pyrolysis conditions (temperature, pressure and heating rate) also affected the properties and reactivity of biomass chars [44], especially the nature and content of inorganics. The low BET surface areas obtained in the present study may be attributed to the presence of AAEMs, which can decrease the surface area by blocking pores [14].

In addition, control experiments (results not shown) with pyrolytic char were carried out to determine the effect of heating, in the absence of steam. Char placed in a nitrogen atmosphere was heated under the same experimental conditions as those obtained from the activation experiments. Under these conditions a substantial reduction in the burn-off was observed at 22.5% and 37.7% at 800 and 900 °C, respectively (Table 2). Under steam gasification, the BET surface areas increased with an increase in the burn-off at various temperatures (Table 2). The extent of the burn-off during char activation significantly increased the surface area of the resulting activated char till reaching a plateau (Fig. 1). The surface areas and total pore volumes of the ACs resulting from heat treatment alone were significantly lower than those of ACs obtained through steam activation, whereas the micropore volumes are slightly higher (Table 2). The activation of char with steam could

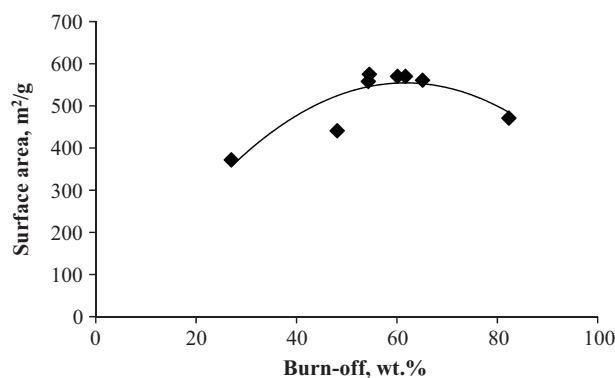


Fig. 1. Optimum burn-off based on BET surface area of the activated carbons at various temperatures.

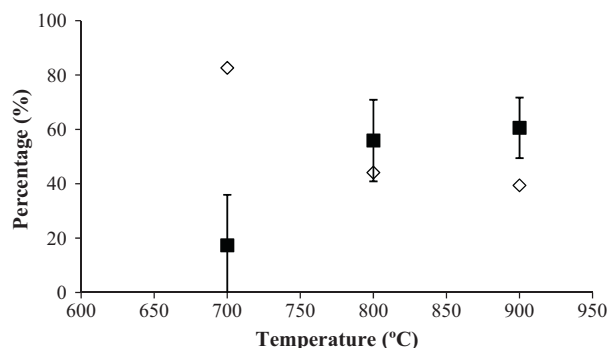


Fig. 2. Distribution of micropores and mesopores + macropores in percent according to the temperature after the vacuum pyrolysis and activation of milled and sieved bagasse: (◇) micropores %; (■) mesopores %.

be associated with additional chemical reactions leading to the removal of carbon atoms and also causing the burn-off, thereby contributing to the development of micropore structure [45] and mesopore structure depending on temperature. To illustrate the change of structure the microporosity and mesoporosity percentages have been plotted against the temperature (Fig. 2). Only the BET surface area increased with an increase in activation temperature whereas the micropore volume decreased (Table 2). This decrease should lead to an increase of mesopore and macropore volumes. The higher temperature apparently caused micropores to widen, by destroying the wall between adjacent pores, thereby resulting in the enlargement of pores by the decrease of micropore volume and an increase in the total pore volume (Table 2) [39]. This last trend was not observed for CO₂ activation leading to the conclusion that CO₂ activation should favor micropore structure development and steam activation macropore and mesopore structure development [46]. Commercially available AC typically have average surface areas of about 1500 m² g⁻¹, although actual values may vary from 400 to over 2000 m² g⁻¹, depending on the

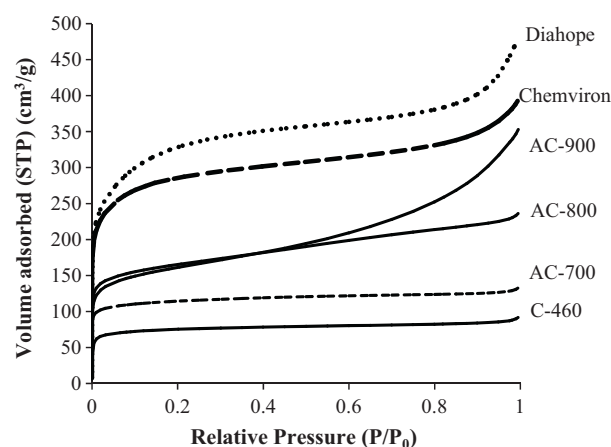


Fig. 3. Influence of steam activation temperature on N₂ adsorption by activated carbons (AC) and chars (C).

degree of burn-off, initial feedstock used and process conditions [39]. Consequently, the ACs produced in this work were in the mid to lower range of AC in terms of surface area, ranging from 391 to 570 m² g⁻¹.

Fig. 3 shows the N₂ adsorption isotherms for the BC and ACs resulting from pyrolysis and steam activation at activation temperatures of 700, 800 and 900 °C respectively. The isotherms corresponding to the biochar after 700 °C-activation are clearly of Type I that are typical of microporous materials whereas the 900 °C-isotherm closely resembles a Type IV isotherm in the Brunauer, Deming and Teller classification consisting of both micro and mesopores, while the 800 °C-isotherm corresponds to a type in between [39]. The flatter the isotherm, the more dominant the micropores [39].

The development of mesoporosity relative to that of microporosity became appreciable at an activation temperature between 700 and 800 °C: the higher the temperature, the steeper the isotherm branches expected at the very low relative pressures (approximately less than the pressure ratio of 0.1) (Fig. 3). This is also evident from the higher values of V₀/V (ratio of micropore volume to total pore volume) of the ACs obtained at 700 °C compared to those obtained at 800 and 900 °C, on average 0.83, 0.44 and 0.32, respectively (Fig. 2).

Table 3 indicates the different pore diameters determined by two different methods (BET and BJH). In general the pore diameters varied in the range of 20–88 Å, indicating a mesoporous–macroporous structure. The pore size of the chars and ACs indicated their potential for use as wastewater adsorbents rather than potential application for gas cleaning [39]. In comparison to a previous study [27], the biochars produced in this study have sufficiently large specific surface areas on which reactions can take place, and a high density of chemical reaction sites where nutrients can be adsorbed [27]. Indeed, Brewer et al.

Table 3
Influence of activation temperature on activated carbon pore diameters from bagasse.

| Bagasse | BET average pore diameter (Å) | BJH ^a adsorption pore diameter (Å) | BJH ^a desorption pore diameter (Å) |
|----------------------------|-------------------------------|---|---|
| C (460 °C) | 21.1 | 58.3 | 35.1 |
| C (900 °C/N ₂) | 20.0–23.0 | 62.8–80.5 | 39.8–56.0 |
| C (800 °C/N ₂) | 19.9 | 73.8 | 44.9 |
| AC (900 °C/Steam) | 30.4–37.5 | 57.4–70.0 | 48.8–60.1 |
| AC (800 °C/Steam) | 25.0–26.1 | 44.2–45.3 | 39.1–39.8 |
| AC (700 °C/Steam) | 20.4 | 45.8 | 34.8 |
| Diahope | 24.5 | 67.5 | 46.6 |
| Chemviron | 24.0 | 60.4 | 48.0 |

^a Barret–Joyner–Halenda (BJH).

Table 4
Influence of the adsorbent type on a MB concentration of a 20 mg l⁻¹.

| Material | MB adsorbed (g/g)-5 min |
|-----------|-------------------------|
| C-460 °C | 4.34 ± 0.15 |
| AC-700 °C | 3.89 ± 0.53 |
| AC-800 °C | 5.22 ± 0.01 |
| AC-900 °C | 5.11 ± 0.08 |
| Diahope | 1.99 ± 0.24 |
| Chemviron | 2.22 ± 0.34 |

[27] determined the BET surface areas of 17 materials varying between 3.3 and 61.6 m² g⁻¹ for corn stover from fast-pyrolysis at 600 °C and switchgrass from steam gasification at 796 °C.

3.1.3. Methylene blue (MB) adsorption

Adsorption from solution is a more complex phenomenon than that of gases since the attraction between the solute and carbon is complicated by forces exerted by the solvent [39]. Table 4 shows the absorbance of MB solution on different materials: the two commercial ACs (Diahope and Chemviron), the char and AC (steam-activated char) produced in the present study. It can be seen that the char and AC from bagasse were better adsorbents for MB than the two commercial ACs. The activation step improved the efficiency of chars in terms of MB adsorption slightly. The ACs obtained from 800 °C and 900 °C activation steps had a higher adsorption efficiency than ones from a 700 °C activation step and commercial granulated ACs.

The addition of SB biochar did not change the pH of the methylene blue solution which is equivalent to pH 5–6. Many researchers studied the effect of initial solution pH on adsorption of methylene blue and concluded that high pH increases the attraction between cations and negatively charged surfaces hence adsorption capacity increased [47–49]. Low adsorption of MB at acidic pH was suggested to be due to the presence of an excess of protons that compete with the dye cation for adsorption sites [23]. Increasing the pH should improve the MB adsorption as the number of positively charged sites decreases while the number of negatively charged sites increases [23].

If the MB adsorption was mainly due to the electrostatic attractions, then their pH of zero point charge (pH_{ZPC}), which controls the repartition between the presence of positive and negative charges on the surface, should be lower for AC-800 and AC-900 for the acidic conditions to improve the affinity between the activated carbon and the cationic dye. Uchimiya et al. [50] showed that an increase in pyrolysis temperature (200–800 °C) led to a loss of oxygen functionality resulting from dehydration, decarboxylation and condensation reactions and higher pH_{ZPC}'s values, which is not in accordance with the previous explanation. Then the slight increase in MB adsorption for AC-800 and AC-900 could be explained by the oxidant treatment of BC through the steam gasification, which should favor the adsorption of polar molecules due to the formation of surface oxygen groups [51]. In addition, the introduction of steam during the activation increased both the BET surface area (Table 2) and enlarged the pore diameter reaching 3.04–3.75 nm, which is larger than the minimum 1.3 nm pore diameter of an adsorbent that MB molecules can enter [52]. This enlargement of pores or the development of mesoporous structures (Fig. 2) by mineral devolatilization apparently improved the adsorption capacities leading to a greater access to the internal surface of adsorbent materials without changing the pH.

The comparison of chars and ACs from vacuum pyrolysis indicated that the char's adsorptive properties were as good as the AC produced from the char by activation at 700 °C. For water treatment applications, the adsorbent obtained from the single step vacuum

Table 5

The pH, surface acidity, surface alkalinity and cation exchangeable capacity of biochar (BC) obtained from vacuum pyrolysis of bagasse.

| Properties | Values |
|--|--------|
| pH(H ₂ O) bagasse | 6.19 |
| pH(H ₂ O) BC | 6.56 |
| pH(KCl) BC | 5.15 |
| Surface acidity (mmol g ⁻¹) | 2.30 |
| Surface alkalinity (mmol g ⁻¹) | 0.31 |
| CEC (cmol _c kg ⁻¹) | 122 |

pyrolysis process could meet all the requirements necessary to be as efficient as some commercial activated carbons (Table 4).

3.2. Characterization of the char as soil amendment

3.2.1. pH, surface acidity, surface alkalinity and FT-IR

The pH of the SB biochar in water is slightly acidic, 6.56 (Table 3). This is in strong contrast to other biochars, which are usually quite alkaline (pH ranging from 7.5 to 9.4) [35,53]. The pH of the biochar in 1 M KCl is more than 1 pH unit lower, which indicated substantial reserve acidity on KCl (neutral salt) exchangeable functional groups. The acidic pH and high degree of exchangeable acidity of the SB biochar could be attributed to its high surface acidity (2.3 mmol g⁻¹) and low surface alkalinity (0.31 mmol g⁻¹) (Table 5).

The surface acidity of the SB biochar is significantly higher than that previously reported for biochar produced from oak wood (0.1 mmol g⁻¹) [36] using slow pyrolysis. The high surface acidity of char indicated a greater content of acidic functional groups such as carboxylic and phenolic groups which are confirmed on the FT-IR spectrum at about 1598 cm⁻¹ and 1092 cm⁻¹, respectively (Fig. 4). On the other hand, the presence of pyrones, carbonates and ash will cause the surface alkalinity [51].

The FT-IR spectrum presented a broad envelope between 1800 cm⁻¹ and 600 cm⁻¹ with sharper bands superimposed on it. The presence of the following functions could explain the intensity at different wave numbers [54]:

- The sharp and intense aromatic ring modes (1700–1500 cm⁻¹) showed the presence of unsaturation such as benzene rings. A search for the out-of-plane C–H bending vibration turns up a band at 798 cm⁻¹ accompanied by a ring-bending at 697 cm⁻¹.
- The presence of C=O stretching vibrations (1800–1600 cm⁻¹) indicated the presence of carboxylic groups and chelated ketones. A search for the C–O stretching vibration (1300–1000 cm⁻¹) indicated two small bands at 1220 cm⁻¹ and 1092 cm⁻¹. These bands

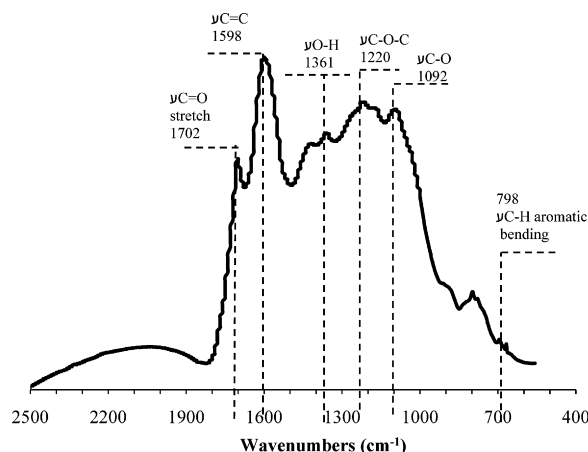
**Fig. 4.** Fourier transform infrared spectrum of SB biochar.

Table 6

Macro and microelements present in the milled and sieved sugar cane bagasse (XRF analysis).

| Element | wt. % |
|---------|-------|
| Al | 0.11 |
| Ca | 0.05 |
| Cr | bd* |
| Fe | 0.17 |
| K | 0.05 |
| Mg | 0.06 |
| Mn | 0.01 |
| Na | bd* |
| P | 0.02 |
| Si | 0.84 |
| Ti | 0.02 |

* bd: below detection.

could be attributed to saturated and asymmetric branched ethers (1210–1070 cm^{-1}).

- The vibrations between 1400 and 1250 cm^{-1} could correspond to the presence of O–H in phenols and carboxylic acids (1361 cm^{-1}).

The pH of the biochar is an important parameter, as it gives an indication of the extent to which the biochar will alter the soil pH, depending on the quantities added. If the pH of the biochar in KCl is lower than that of the soil, it will most likely lower the soil pH, in relation to the quantities applied. This could be of benefit to slightly acidic to alkaline soils, and would enhance nutrient availability [28,29]. A soil pH level of around 6.3–6.8 is the optimum range in terms of nutrient availability for most plants and is preferred by most beneficial soil bacteria [55].

The pH of the carbonization products can be used as an important parameter to evaluate the surface properties of biochar such as surface electrical charge and volatiles, which depends on the presence of ash [14]. One of the important features of biomass materials is the presence of significant amounts of alkali and AAEM species (mainly K, Na, Mg and Ca) in the biomass (Table 6). These AAEM species tend to volatilise during pyrolysis (and gasification/combustion). The presence of AAEM can decrease the surface area by blocking pores and render the surface more alkaline at high temperature [14]. This phenomenon was illustrated by the slight increase of pH (0.3 pH units) between the raw bagasse and biochar produced at 460 °C (Table 5).

3.2.2. Cation exchange capacity (CEC)

The CEC is used to describe the potential of biochar to reversibly adsorb positively charged species (i.e. they are exchangeable and readily available for plants to absorb) [27]. The CEC is a function of the presence of hard ligand functional groups in the char such as carboxyl and phenolic groups [29]. The CEC of the SB biochar (122 $\text{cmol}_c \text{kg}^{-1}$) was relatively high and significantly higher than the CEC previously reported for biochar produced from paper mill waste (9–18 $\text{cmol}_c \text{kg}^{-1}$) [53] using slow pyrolysis, although similar to the CEC reported for crop straw biochars (100–300 $\text{cmol}_c \text{kg}^{-1}$) [55]. The CEC of the SB biochar (122 $\text{cmol}_c \text{kg}^{-1}$) was similar to that of the common soil minerals montmorillonite (70–95 $\text{cmol}_c \text{kg}^{-1}$) and dioctahedral vermiculite (100–150 $\text{cmol}_c \text{kg}^{-1}$). It was much higher than that of kaolinite (3–15 $\text{cmol}_c \text{kg}^{-1}$), which is the typical clay mineral found in Mediterranean regions such as the Western Cape (South Africa) [56]. However, the CEC of the SB biochar was somewhat lower than the typical CEC values reported for soil organic matter (humus) (200 $\text{cmol}_c \text{kg}^{-1}$) [56].

The relatively high CEC of the biochar could be attributed to its high surface acidity (Table 5), and indicated that the SB biochar could be a very good exchange medium for cationic macro- and micronutrients, and could thereby enhance the nutrient holding capacity of soils, an important measure of soil fertility [28].

Table 7

Water soluble ions (mg kg^{-1}) extracted from the biochar and the EC (dS m^{-1}) of the water extract.

| Ions | mg kg^{-1} |
|--|---------------------|
| Ca^{2+} | 32 |
| Mg^{2+} | 25 |
| Na^{+} | 173 |
| K^{+} | 560 |
| F^{-} | 2 |
| Cl^{-} | 84 |
| PO_4^{3-} | 317 |
| SO_4^{2-} | 335 |
| NO_3^{-} | 0 |
| NO_2^{-} | 0 |
| Electrical Conductivity dS m^{-1} | 0.17 |

The combination of the high level of surface oxidation from the low pyrolysis temperature (Table 2) and the high BET surface area would make biochar less resistant to chemical oxidation and microbial degradation, and hence shorten the half-life in soils, compared to biochars produced at higher temperature [38]. Nevertheless, the biochar produced at low temperatures was more able to increase soil CEC values due to the combination of a high BET surface area and charge density [34].

3.2.3. Electrical conductivity (EC) and water-soluble ions

The EC value is a measure of the total water-soluble ions (salinity) present in the biochar, which can negatively affect plant growth if very high, leading to a decrease in water uptake by plant roots and nutrient imbalances [30]. The SB biochar had a relatively low EC of 0.17 dS m^{-1} (Table 6), similar to the values reported for Eucalyptus biochar (0.09–0.17 dS m^{-1}) [57]. Generally, a measured EC above 4 dS m^{-1} in a soil water extract indicates saline soil. Thus, the low salinity content of the SB biochar, as indicated by the low EC, indicated that soil application of the SB biochar should not have a significant negative impact on soil salinity.

The water soluble ions in the biochar (Table 7) give an indication of readily available plant nutrients in the biochar. Nitrogen, P, K, Ca, Mg and S are considered the universally essential plant macronutrients [58]. Sodium is not considered as an essential plant nutrient, and has negative effects on soil structure by promoting clay dispersion [58]. Plants only use inorganic forms of N (ammonium and nitrate), P (phosphate) and S (sulfate) as nutrients from soils [30]. Thus the added benefit of using a water extract is that ion chromatography can be used to quantitatively determine the concentrations of inorganic N, P and S anionic species which are among the most important nutrients for plants [30].

The Ca and Mg concentrations are much lower than that of K and Na in the water extract (Table 7) while the total concentrations are similar (Table 8). This can be attributed to the fact that K and Na carbonates and oxides are much more soluble in water than the corresponding Ca and Mg compounds [59]. These basic cation carbonates and oxides tend to form in the ash fraction of the char (Table 1). The water soluble phosphate and sulfate concentrations of the biochar are relatively high, which would be beneficial to plant growth [28]. The water soluble phosphate concentration is high due to the relatively acidic pH of the char, which makes it the most readily available as opposed to being co-precipitated with Ca or Mg under alkaline conditions. The char contains little or no NO_3^{-} which is a vital plant nutrient, and thus it is highly recommended that N fertilizer be supplemented when applying the biochar [60]. In comparison to biochar, a commercial NPK fertilizer such as 2:3:4 (30) contains water soluble nutrients at the following levels: 67 g N kg^{-1} , 100 g P kg^{-1} and 133 g K kg^{-1} [60]. Thus, the biochar cannot be considered as a balanced fertilizer, as it contains relatively low levels of water soluble nutrients and is lacking the most vital nitrogen element. The absence of any detectable nitrites

Table 8

Plant available nutrients and non-essential elements in the biochar (1% citric acid extraction).

| Element | Concentrations (mg kg ⁻¹) | Authorized limit (mg kg ⁻¹) |
|-----------------------------------|---------------------------------------|---|
| Macro and micro nutrients | | |
| P | 451 | |
| Ca | 2181 | |
| Mg | 1158 | |
| K | 3464 | |
| Fe | 3953 | |
| Mn | 162 | |
| Zn | 42 | 7500 |
| Cu | 9 | 4300 |
| Co | 1.9 | |
| Mo | 0.01 | |
| Non-essential elements and toxins | | |
| Na | 48.70 | |
| As | 0.41 | 75 |
| Cd | 0.03 | 85 |
| Cr | 13.00 | 3000 |
| Pb | 3.60 | 840 |
| Ni | 4.49 | 420 |
| Se | n/d | 100 |

and nitrates in the biochar water extract (Table 7) indicates that the low amount of N detected by elemental analysis (Table 1) is probably in the form of condensed, heterocyclic-N containing structures [61]. Thus, the nitrogen in the biochar is mostly in a recalcitrant, plant-unavailable form [34].

3.2.4. Citric acid-extractable nutrients

The SB biochar contained moderate amounts of the essential plant nutrient, P (451 mg kg⁻¹), as well as substantial amounts of plant-available macronutrients, K, Ca and Mg (3.46, 2.18 and 1.16 g kg⁻¹, respectively) (Table 8). The biochar also contained a remarkably high amount of Fe (3.95 g kg⁻¹). This is most likely due to the treatment process of the sugar cane, and is not likely to be due to the uptake of Fe by the sugar cane plant during its normal growth process. The high concentration of iron could be due to the treatment of sugar cane bagasse by ferrous sulfate used against disease [62]. In addition, the presence of this iron could be explained by the preparation process, where the knives and hammers wear, and some iron is picked up by corrosion of the steelwork by the slightly acidic juice (pH around 5.0). The SB biochar also contained trace amounts of plant micronutrients, Mn, Zn, Cu, Co and Mo (Table 8). Based on the usual recommended biochar application rate of 10 tonnes per hectare [30], the SB biochar should be able to supply half of the K, Ca, and Mg and a tenth of the P requirement of a crop such as wheat. The plant-available toxic elements such as As, Cr, Pb and Cd are present in trace amounts and are below the authorized limits for organic soil amendments [63].

4. Conclusions

This study focussed on the potential of char from the vacuum pyrolysis of sugar cane bagasse (460 °C, 8 kPa, 17 °C min⁻¹) as an activated carbon and a soil amendment. The analyses used to describe adsorption and soil amendment qualities highlighted the high potential of char from bagasse to decolorize wastewaters and increase the soil nutrient levels and nutrient holding capacity.

For the adsorption of cationic dyes the performance of char from vacuum pyrolysis was equivalent to that of activated carbons produced by steam gasification of the same materials, implying that the activation step was not essential for this application. The extended study on the porous structure of the raw and activated chars, using BET surface area determination, pointed out the greater development of meso and macropore structures in both materials, which appears mainly to be involved in MB's adsorption. In addition,

the importance of the chemical nature of the char's surface has been pointed out and should be composed of negatively charged functional groups that retain MB by electrostatic attractions. The determination of pH in water and salt solutions, surface acidity, FT-IR spectroscopic analysis and CEC confirm the presence of negatively charged, hard Lewis ligand functional groups in the char such as carboxyl groups.

Moreover the adsorption properties make the biochar an excellent exchange medium for cationic plant macro- and micronutrients. The relatively high CEC of the biochar (122 cmol_c kg⁻¹) was similar to that of reactive soil clays such as vermiculite and montmorillonite. In addition, the biochar from the pyrolysis of sugar cane bagasse was slightly acidic, a remarkable property considering that the majority of reported biochars are alkaline. This indicated that the biochar is already at the optimum pH for plants and microbes in soils, making it a much more widely useable biochar than the alkaline biochar. The biochar was also a good source of beneficial plant macro- and micronutrients and contained negligible levels of toxic elements. Unfortunately, the biochar could not be considered as a balanced fertilizer on its own, as it contains relatively low levels of water soluble nutrients and is lacking the most vital element, N. Therefore, it should be applied together with an NPK fertilizer when using it as a soil amendment. The highly porous nature of the biochar, especially the micro and mesoporosity, indicated that the biochar would effectively improve the water retention in soils [64], which is especially desirable in sandy soils. Plants can only take up nutrients if the soil is wet, so this would also contribute to improved nutrient uptake in a soil. Furthermore the microporous structure would serve as an excellent, moist habitat for soil microorganisms [65].

Acknowledgments

The authors gratefully acknowledge Prof. Hein Neomagus for the use of the activation equipment at North-West University, South Africa. The authors also wish to thank the Sugar Milling Research Institute for supply of sugar cane bagasse for the study and Steve Davis for his inputs. The BET analyses, elemental analyses and ICP-MS measures were performed by Hanlie Botha, Esmé Spicer and Matt Gordon and Riana Rossouw, respectively.

References

- [1] K. Deepchand, Sugar Cane Bagasse Energy Cogeneration – Lessons from Mauritius, Paper Presented to the Parliamentarian Forum on Energy Legislation and Sustainable Development, Cape Town, South Africa, 5–7 October 2005.
- [2] Energy statistics database, www.data.un.org, 28 August 2008.
- [3] N.H. Leibbrandt, J.H. Knoetze, J.F. Görgens, Comparing biological and thermochemical processing of sugarcane bagasse: an energy balance perspective, *Biomass and Bioenergy* 35 (5) (2011) 2117–2126.
- [4] A.R. Gonçalves, D.S. Ruzene, R.Y. Moriya, L.R.M. Oliveria, Pulping of sugarcane bagasse and straw and biobleaching of the pulps: conditions parameters and recycling of enzymes, in: 59th Appita Conference, Auckland, New Zealand, 16–19 May, 2005, 2005.
- [5] P.B. Devnarain, Production of activated carbon from South African sugar-cane bagasse, MSc (Eng) Thesis, University of KwaZulu-Natal, 2003.
- [6] D. Mwasisebe, B.Eng. Thesis, Production of Activated carbon from south African sugarcane bagasse, University of KwaZulu-Natal, 2005.
- [7] D. Diedericks, E. van Rensburg, M. del Prado García-Aparicio, J.F. Görgens, Enhancing of the enzymatic digestibility of sugarcane bagasse through the application of an ionic liquid in combination with an acid catalyst, *Biotechnology progress* 28 (1) (2012) 76–84.
- [8] M. Carrier, T. Hugo, J. Görgens, J.H. Knoetze, Comparison of slow and vacuum pyrolysis of sugar cane bagasse, *Journal of Analytical and Applied Pyrolysis* 90 (2011) 18–26.
- [9] N.S. Mamphweli, E.L. Meyer, Evaluation of the conversion efficiency of the 180 Nm³/h Johansson Biomass Gasifier™, *International Journal of Energy and Environment* 1 (1) (2010) 113–120.
- [10] A.V. Bridgewater, Renewable fuels and chemicals by thermal processing of biomass, *Chemical Engineering Journal* 91 (2003) 87–102.
- [11] International Energy Agency, Sustainable production of second-generation bio-fuels: potential and perspectives in major economies and developing countries, <http://www.iea.org>, date of access: 18 August 2010.

- [12] W.T. Tsai, M.K. Lee, Y.M. Chang, Fast pyrolysis of rice straw, sugarcane bagasse and coconut shell in an induction-heating reactor, *Journal of Analytical and Applied Pyrolysis* 76 (2006) 230–237.
- [13] S. Al Arni, B. Bosio, E. Arato, Syngas from sugarcane pyrolysis: an experimental study for fuel cell applications, *Renewable Energy* 35 (2010) 29–35.
- [14] Y. Shinogi, Y. Kanri, Pyrolysis of plant, animal and human waste: physical and chemical characterization of pyrolytic products, *Bioresource Technology* 90 (2003) 241–247.
- [15] P. Das, A. Ganesh, P. Wangikar, Influence of pretreatment for deashing of sugarcane bagasse on pyrolysis products, *Biomass and Bioenergy* 27 (2004) 445–457.
- [16] M. Garcia-Perez, A. Chaala, C. Roy, Co-pyrolysis of sugarcane bagasse with petroleum residue. Part II. Production yields and properties, *Journal of Analytical and Applied Pyrolysis* 65 (2002) 111–136.
- [17] K.A. Krishnan, T.S. Anirudhan, Uptake of heavy metals in batch systems by sulfurized steam activated carbon prepared from sugarcane bagasse pith, *Industrial & Engineering Chemistry Research* 41 (2002) 5085–5093.
- [18] M. Ahmedna, W.E. Marshall, R.M. Rao, Production of granular activated carbons from select agricultural by-products and evaluation of their physical, chemical and adsorption properties, *Bioresource Technology* 71 (2000) 103–112.
- [19] E.C. Bernardo, R. Egashira, J. Kawasaki, Decolorization of molasses' wastewater using activated carbon prepared from cane bagasse, *Carbon* 35 (1997) 1217–1221.
- [20] B.P. Lavarack, Chemically activated carbons from sugarcane bagasse fractions, *Hungarian Journal of Industrial Chemistry* 25 (1997) 157–160.
- [21] M. Ruiz, C. Rolz, Activated carbons from sugar cane bagasse, *Industrial & Engineering Chemistry Product Research and Development* 10 (1971) 429–432.
- [22] A.R. Zimmerman, Abiotic and microbial oxidation of laboratory-produced black carbon (biochar), *Environmental Science & Technology* 44 (2010) 1295–1301.
- [23] M. Rafatullah, O. Sulaiman, R. Hashim, A. Ahmad, Adsorption of methylene blue on low-cost adsorbents: a review, *Journal of Hazardous Materials* 177 (2010) 70–80.
- [24] O. Hamdaoui, Batch study of liquid-phase adsorption of methylene blue using cedar sawdust and crushed brick, *Journal of Hazardous Materials B* 135 (2006) 264–273.
- [25] A. Ahmad, M. Rafatullah, O. Sulaiman, M.H. Ibrahim, R. Hashim, Scavenging behaviour of meranti sawdust in the removal of methylene blue from aqueous solution, *Journal of Hazardous Materials* 170 (2009) 357–365.
- [26] S.D. Joseph, M. Camps-Arbestain, Y. Lin, P. Munroe, C.H. Chia, J. Hook, L. van Zwieten, S. Kimber, A. Cowie, B.P. Singh, J. Lehmann, N. Foidl, R.J. Smernik, J.E. Amonette, An investigation into the reactions of biochar in soil, *Australian Journal of Soil Research* 48 (2010) 501–515.
- [27] C.E. Brewer, R. Rachel Unger, K. Schmidt-Rohr, R.C. Brown, Criteria to select biochars for field studies based on biochar chemical properties, *Bioenergy Research*, doi:10.1007/s12155-011-9133-7.
- [28] B. Glaser, J. Lehmann, W. Zech, Ameliorating physical and chemical properties of highly weathered soils in the tropics with charcoal—a review, *Biology and Fertility of Soils* 35 (2002) 219–230.
- [29] J.D. Rhoades, Cation exchange capacity, in: A.L. Page, et al. (Eds.), *Methods of Soil Analysis, Part 2: Chemical and Microbiological Properties*, ASA and SSSA, Madison, WI, 1982.
- [30] K.Y. Chan, L. Van zwieten, I. Meszaros, A. Downie, S. Joseph, Agronomic values of green waste biochar as a soil amendment, *Australian Journal of Soil Research* 45 (2007) 629–634.
- [31] T.H. De Luca, M.D. MacKenzie, M.J. Gundale, Biochar effects on soil nutrient transformations, in: J. Lehmann, S. Joseph (Eds.), *Biochar for Environmental Management. Science and Technology*, Earthscan, London, 2009, pp. 251–270.
- [32] F.X. Yao, M. Camps Arbertain, S. Virgel, F. Blanco, J. Arostegui, J.A. Maciá-Agulló, F. Macías, Simulated geochemical weathering of a mineral ash rich biochar in a modified Soxhlet reactor, *Chemosphere* 80 (2010) 724–732.
- [33] J.H. Potgieter, C.A. Strydom, Determination of the clay index of limestone with methylene blue adsorption using a UV–vis spectrophotometric method, *Cement and Concrete Research* 29 (1999) 1815–1817.
- [34] C.E. Brewer, K. Schmidt-Rohr, J.A. Satrio, R.C. Brown, Characterization of biochars from Fast Pyrolysis and Gasification systems, *Environmental Progress & Sustainable Energy* 28 (3) (2009) 386–396.
- [35] J.F. Novak, W.J. Busscher, D.L. Laird, M. Ahmedna, D.W. Watts, M.A.S. Niandou, Impact of biochar amendment on fertility of a Southeastern coastal plain soil, *Soil Science* 174 (2009) 105–112.
- [36] C.H. Cheng, J. Lehmann, Ageing of black carbon along a temperature gradient, *Chemosphere* 75 (2009) 1021–1027.
- [37] F.J. Stevenson, *Humus Chemistry: Genesis, Composition, Reactions*, John Wiley & Sons, New York, USA, 1994.
- [38] J. Lehmann, Bio-energy in the black, *Frontiers in Ecology and the Environment* 5 (2007) 381–387.
- [39] R.C. Bansal, J.-B. Donnet, F. Stoeckli, *Active Carbon*, Marcel Dekker Inc., New York and Basel, 1988.
- [40] J.G. Olsson, U. Jaglid, J.B.C. Pettersson, P. Hald, Alkali metal emission during Pyrolysis of biomass, *Energy & Fuels* 11 (1997) 779–784.
- [41] O. Hirohata, T. Wakabayashi, K. Tasaka, C. Fushimi, T. Furusawa, P. Kuchonthara, A. Tsutsumi, Release behaviour of tar and alkali and alkaline earth metals during biomass steam gasification, *Energy and Fuels* 22 (6) (2008) 4235–4239.
- [42] A. Smolinski, N. Howaniec, K. Stanczyk, A comparative experimental study of biomass, lignite and hard coal steam gasification, *Renewable Energy* 36 (2011) 1836–1842.
- [43] E.F. Jaguaribe, L.L. Medeiros, M.C.S. Barreto, L.P. Araujo, The performance of activated carbons from sugarcane bagasse, babassu, and coconut shells in removing residual chlorine, *Brazilian Journal of Chemical Engineering* 22 (2005) 41–47.
- [44] A.C. Lua, T. Yang, Effects of vacuum pyrolysis conditions on the characteristics of activated carbons derived from pistachio-nut shells, *Journal of Colloid and Interface Science* 276 (2004) 364–372.
- [45] S. Luo, B. Bo Xiao, Z. Hu, S. Liu, X. Guo, M. He, Hydrogen-rich gas from catalytic steam gasification of biomass in a fixed bed reactor: influence of temperature and steam on gasification performance, *International Journal of Hydrogen Energy* 34 (2009) 2191–2194.
- [46] T. Zhang, W.P. Walawender, L.T. Fan, M. Fan, D. Daugaard, R.C. Brown, Preparation of activated carbon from forest and agricultural residues through CO₂ activation, *Chemical Engineering Journal* 105 (2004) 53–59.
- [47] F.A. Batzias, D.K. Sidiras, Simulation of methylene blue adsorption by salts-treated beech sawdust in batch and fixed-bed systems, *Journal of Hazardous Materials* 149 (1) (2007) 8–17.
- [48] N. Nasuha, B.H. Hameed, A.T.M. Din, Rejected tea as potential low-cost adsorbent for the removal of methylene blue, *Journal of Hazardous Materials* 175 (2010) 126–132.
- [49] O. Gerçel, A. Özcan, A. Safa Özcan, H. Ferdi Gerçel, Preparation of activated carbon from a renewable bio-plant of Euphorbia rigida by H₂SO₄ activation and its adsorption behavior in aqueous solutions, *Applied Surface Science* 253 (2007) 4843–4852.
- [50] M. Uchimiya, L.H. Wartelle, K.T. Klasson, C.A. Fortier, I.M. Lima, Influence of pyrolysis temperature on biochar property and function as a heavy metal sorbent in soil, *Journal of Agricultural and Food Chemistry* 59 (2011) 2501–2510.
- [51] G. Finqueneisel, T. Zimny, A. Albinak, T. Siemieniowski, D. Vogt, J.V. Weber, Cheap adsorbent Part 1: active cokes from lignites and improvement of their adsorptive properties by mild oxidation, *Fuel* 77 (6) (1998) 549–556.
- [52] S. Gaspard, S. Altenor, E.A. Dawson, P.A. Barnes, A. Ouensanga, Activated carbon from vetiver roots: gas and liquid adsorption studies, *Journal of Hazardous Materials* 144 (2007) 73–81.
- [53] L. Van Zwieten, S. Kimber, S. Morris, K.Y. Chan, A. Downie, J. Rust, S. Joseph, A. Cowie, Effects of biochar from slow pyrolysis of papermill waste on agronomic production and soil fertility, *Plant Soil* 327 (2010) 235–246.
- [54] U.M. Garg, M.P. Kaur, V.K. Garg, D. Sud, Removal of hexavalent chromium from aqueous solution by agricultural waste biomass, *Journal of Hazardous Materials* 140 (2007) 60–68.
- [55] K.H. Tan, *Principles of Soil Chemistry*, CRC Press, Boca Raton, FL, 2010.
- [56] J.-H. Yuan, R.-K. Xu, H. Zhang, The forms of alkalis in the biochar produced from crop residues at different temperatures, *Bioresource Technology* 102 (3) (2011) 3488–3497.
- [57] B.P. Singh, B.J. Hatton, B. Singh, A.L. Cowie, A. Kathuria, Influence of biochars on nitrous oxide emission and nitrogen leaching from two contrasting soils, *Journal of Environmental Quality* 39 (2010) 1224–1235.
- [58] J.L. Havlin, J.D. Beaton, S.L. Tisdale, W.L. Nelson, *Soil Fertility and Nutrient Management: An Introduction to Nutrient Management*, 7th ed., Pearson/Prentice Hall, Upper Saddle River, NJ, 2005, 515 pp.
- [59] M.B. McBride, *Environmental Chemistry of Soils*, Oxford University Press, London, UK, 1994.
- [60] FSSA (Fertilizer Society of South Africa), *FSSA Fertilizer Handbook*, The Fertilizer Society of South Africa, Pretoria, 2007.
- [61] S. Koutcheiko, C.M. Monreal, H. Kodama, T. McCracken, L. Kotlyar, Preparation and characterization of activated carbon derived from the thermo-chemical conversion of chicken manure, *Bioresource Technology* 98 (2007) 2459–2464.
- [62] A. Dametie, T. Mamo, S. Zelleke, Studies on iron chlorosis of sugar cane (*Saccharum officinarum* L.) at metahara, Ethiopia: soil and plant characterisation and efficiency of different iron sources, *Journal of Agronomy and Crop Science* 175 (1995) 317–324.
- [63] U.S. EPA, Clean Water Act, sec. 503, no. 32, vol. 58, U.S. Environmental Protection Agency, Washington, D.C., 1993.
- [64] D. Hillel, *Environmental Soil Physics*, Academic Press, USA, 1998.
- [65] J.E. Thies, M.C. Rillig, Characteristics of biochar: biological properties, in: J. Lehmann, S. Joseph (Eds.), *Biochar for Environmental Management: Science and Technology*, Earthscan, London, UK, 2009.